

One Methylene Group in the Side Chain Can Alter by 90 Degrees the Orientation of a Main-Chain Liquid Crystal on an Unidirectional Substrate

Yaroslav Odarchenko,^{a†} Matthieu Defaux,^a Martin Rosenthal,^{a‡} Azaliia Akhiamova,^{b,c} Polina Bovsunovskaya,^{b,c} Alexey Melnikov,^{b,c} Alexander Rodygin,^{b,c} Andrey Rychkov,^{b,c} Kirill Gerasimov,^{b,c} Denis V. Anokhin,^{b,c,d} Xiaomin Zhu^e and Dimitri A. Ivanov^{a, b, c}

^a Institut de Sciences des Matériaux de Mulhouse-IS2M, CNRS UMR 7361 Jean Starcky, 15, F-68057 Mulhouse, France E-mail: Dimitri.Ivanov@uha.fr

^b Lomonosov Moscow State University, Faculty of Fundamental Physical and Chemical Engineering, Leninskie Gory 1/51, 119991, Moscow, Russian Federation

^c Moscow Institute of Physics and Technology (State University), Institutskiy per. 9, Dolgoprudny, 141700, Russian Federation

^d Institute of Problems of Chemical Physics, Russian Academy of Sciences, Chernogolovka, Moscow oblast, 142432, Russian Federation

^e DWI – Leibniz-Institute for Interactive Materials e.V. and Institute for Technical and Macromolecular Chemistry of RWTH Aachen University, Forckenbeckstr. 50, D-52056 Aachen, Germany.

KEYWORDS alignment, confinement, epitaxy, liquid-crystalline polymer, poly(*di-n* alkylsiloxane).

ABSTRACT: The mechanisms of orientation of columnar liquid crystals (LCs) on PTFE-rubbed surface are explored on a homologous series of symmetrically-substituted poly(*di-n*-alkylsiloxanes) (PDAS). It is shown that by increasing the side-chain length in steps of one CH₂ group the orientation of PDAS switches back and forth from perpendicular to parallel with respect to PTFE chains. These changes sensitive to the smallest possible variation of the macromolecular structure (i.e., modification of the side chain length by just one CH₂ group) reflect the change of the alignment mechanism identified as grapho-epitaxial or epitaxial for the perpendicular and parallel orientation, respectively. The results show that two orthogonal LC orientations are realizable on the same rubbed substrate, which can open new perspectives in the field of organic and printed electronics such as multi-domain LCD technology.

Control of the liquid crystals' (LCs) orientation is essential for a variety of practical applications such as liquid crystal displays (LCD),¹ field-effect transistors,² optically active coatings and sensors.^{3,4} The LCD market has fully appreciated the advantages of LC state of matter combining order and mobility that allow for low-power consumption, high efficiency, low cost and device compactness. A uniform LC alignment can be induced with the help of inhomogeneous surfaces⁵, patterned substrates⁶⁻⁹, a variety of external fields (e.g. magnetic^{10,11}, electric¹² or mechanical¹³) or by using porous templates.^{14,15} Among other alignment methods, buffing of the substrate coated with a polymer has attracted a particular attention for its relative simplicity and low cost. This LC alignment method has been adopted industrially and is extensively used in fabrication of optical and polarizing films and LCD displays. Despite intense research efforts, the detailed mechanism of the LC alignment by polymer buffing is still a matter of debate.¹⁶ According to the literature, the most probable explanation is the existence of microgrooves created while buffing the polymer surface.^{6,7,17} In the other words, orientation of the LC phases occurs via grapho-epitaxy. This method has also several disadvantages such as

sensitivity to scratches on the alignment surface, dust generation from cloths or synthetic fibers and static electricity resulting in display defects.^{18,19}

A promising way to prepare highly-oriented and molecularly smooth semicrystalline polymer layers on rubbed polytetrafluoroethylene (PTFE) was proposed by Wittmann and Smith.²⁰ Rigidity, stability and high melting temperature of PTFE could potentially make this method efficient for optical LC films including displays. Yet, up to date the literature reports concerned almost exclusively semicrystalline polymers and low-molecular-weight organic crystals epitaxially grown on PTFE-rubbed substrates.²¹⁻²³ In most cases the thin-film alignment was explained by the lattice matching in the contact planes of the growing crystal and PTFE. Generally, molecular epitaxy is a well-studied phenomenon for conventional solid crystals, but, to the best of our knowledge, was only scarcely discussed for LC phases. Thus, the alignment mechanism similar to that known for 3D crystals was suggested for smectic and nematic LCs based on optical microscopy data.²⁴ However, no information about lattice mismatch of the polymer substrate and deposited LC has been provided.

In this study, we show that the mechanism of spontaneous orientation of columnar LC polymers on PTFE-rubbed substrates can alternate between molecular epitaxy and grapho-epitaxy. To explore the mechanisms of the LC orientation, we use a unique homologous series of main-chain columnar poly(di-*n*-alkylsiloxane)s (PDAS) with *n* ranging from 2 to 6.²⁵ By increasing the length of the alkyl side chain of these symmetrically-substituted PDAS in steps of one CH₂ group, we explore

in detail the impact of the mismatch between the LC lattice and PTFE-rubbed surface on the polymer orientation. For the sake of comparison, the molecular orientation is also addressed for PDAS embedded in nanoporous templates in which no epitaxial interaction is expected.

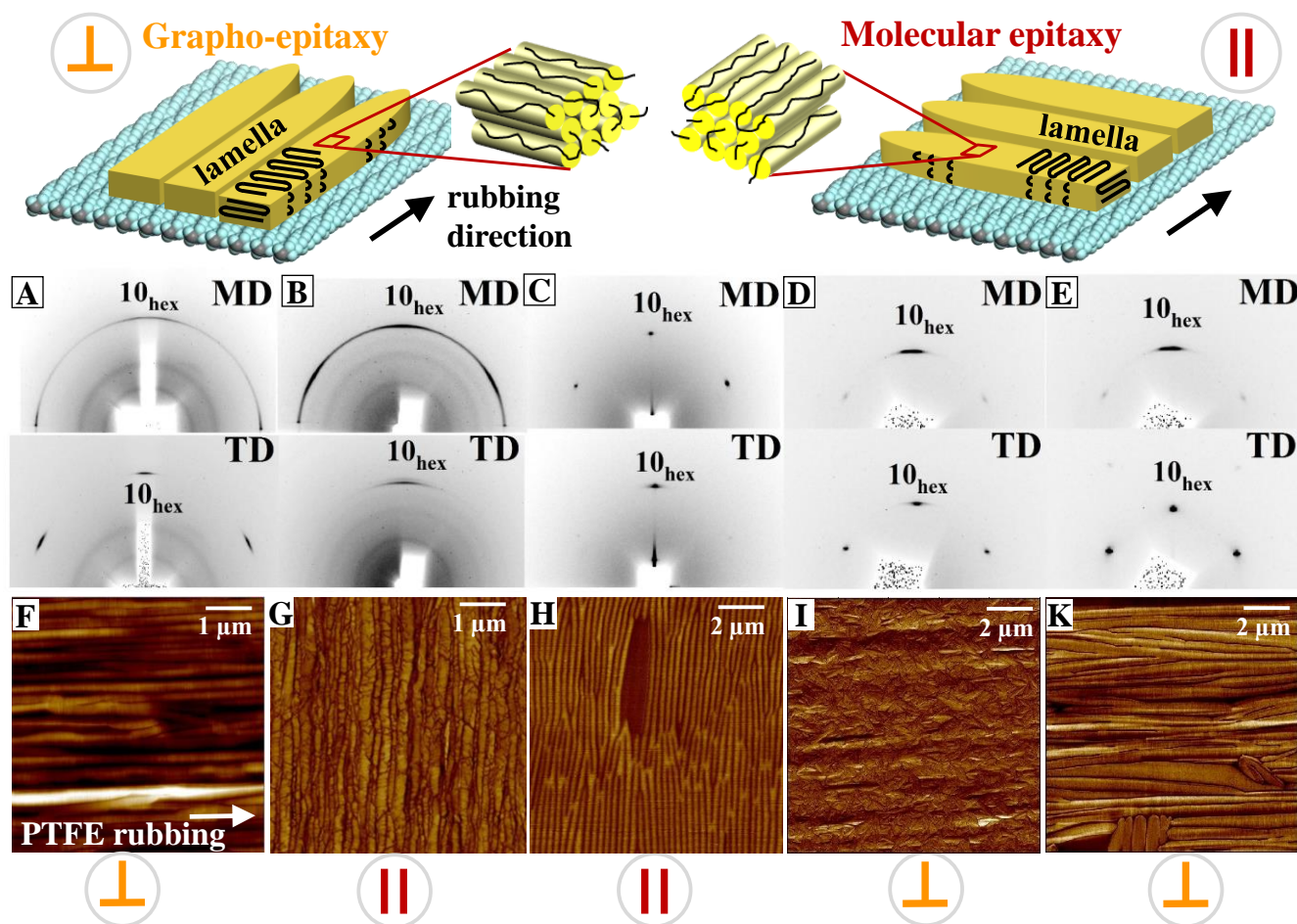


Figure 1. *Top:* schematic representation of the two mutually orthogonal orientations of the PDAS backbones on a PTFE-rubbed substrate, which are due to the grapho-epitaxial (\perp) and epitaxial (\parallel) orientation mechanisms. *Bottom:* 2D GIWAXS patterns of PDES (A), PDPS (B), PDBS (C), PDPenS (D) and PDHS (E) thin films deposited on PTFE-rubbed surface measured in the machine (MD) and transversal (TD) directions. AFM Tapping Mode micrographs of PDES (F), PDPS (G), PDBS (H), PDPenS (I) and PDHS (K) showing lamellae (needle-like objects) grown on a PTFE-rubbed surface. The PTFE rubbing direction is close to horizontal (indicated with the white arrow). The orientation of the backbones is indicated for each of the studied PDAS with respect to PTFE chains. All measurements were conducted at room temperature except GIWAXS for PDPS, which was performed at 90 °C.

The polymer film texture is studied with a combination of grazing-incidence and micro-focus X-ray diffraction (GIXD and μ XRD, respectively) and Atomic Force Microscopy (AFM).

The family of liquid-crystalline PDAS starts with poly(diethylsiloxane) (PDES, *n*=2) because PDMS is semicrystalline. PDES has a mesophase stability window from -10 to 53 °C (cf. Table S1); it forms tapered-edge lamellae that have been described elsewhere.²⁶ An AFM micrograph of PDES on a PTFE-rubbed substrate shows well-oriented lamellae with their long axis parallel to rubbing direction (cf. Figure 1F). Taking into account that polymer chains are perpendicular to the long lamellar axis,^[28] the PDES backbone is therefore perpendicular to the rubbing direction. This is confirmed by

GIXD in the machine (MD) and transversal (TD) directions (cf. Figure S1), where MD corresponds to the rubbing direction and TD is perpendicular to it. In the MD pattern, the maximum intensity of 10 peak of a hexagonal mesophase is positioned on the meridian (cf. Figure 1A), whereas in the TD pattern, the 10 reflections with equal intensities are observed at 60 ° with respect to each other. This provides evidence that (hk) plane of the hexagonal PDES lattice is parallel to rubbing. The resulting PDES film structure is schematically depicted in Figure 1 (top left). It is thus clear that orientation of PDES is defined by substrate topography and not by mismatch of the unit cells, which means that it is the case of grapho-epitaxy.

When one methylene group is added to the side chain, *i.e.* one passes from PDES to poly(dipropylsiloxane) (PDPS, $n=3$),^{27,28} the backbone orientation changes by 90° and becomes parallel to rubbing.²⁶ This can be concluded from the corresponding GIXD pattern (cf. Figure 1B). The increase of the intercolumnar distance from 9.3 to 11.2 Å is in line with expansion of the PDPS column diameter compared to PDES (cf. Table 1). The orientation of PDPS is preserved upon crystallization, as can be seen from the room-temperature AFM micrographs showing lamellae oriented perpendicular to the rubbing direction (cf. Figure 1G). Therefore, the PDES and PDPS orient differently on PTFE, as schematically depicted in the top right panel of Figure 1. The other polymers of the

PDAS family with longer side-chains, *i.e.* poly(dibutylsiloxane) (PDBS), poly(dipentylsiloxane) (PDPenS) and poly(dipentyl/hexyl-siloxane) copolymer with monomer ratio of 10/90 (denoted as PDHS) exhibit LC state over a wide temperature range including room temperature (cf. Table S1). For PDBS with $n=4$ the columnar diameter increases to 10.65 Å while the orientation of the chains on the PTFE-rubbed substrate is kept the same as for PDPS (cf. Figure 1C,H). Further increase of n to 5 results in a backward switch of orientation. Despite the fact that the corresponding AFM images reveal numerous defects in the film organization, the PDPenS lamellae orientation is clearly visible (Figure 1I).

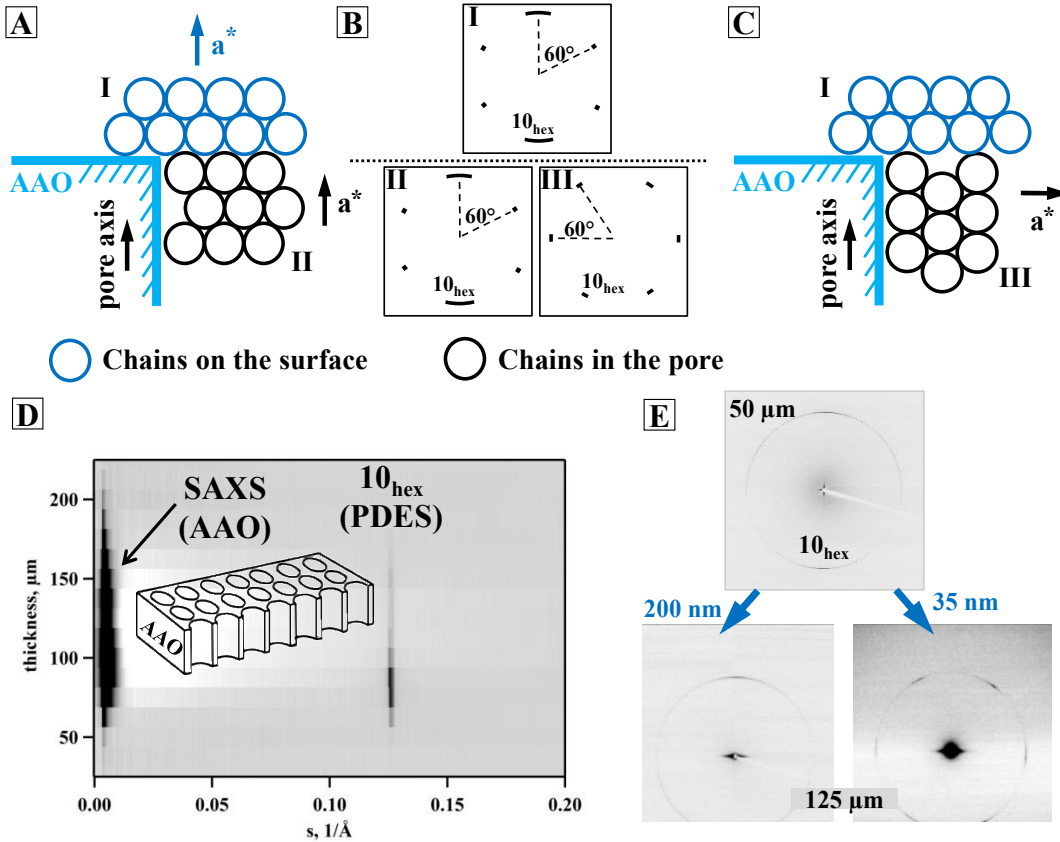


Figure 2. *Top:* cartoon showing two different orientations of the PDAS lattice for the geometrically confined PDAS. The case of 200 nm-sized pores is depicted in (A) while that of the 35 nm-sized pores- in (C). The layers formed by PDAS in the 200 nm pores can be viewed as being perpendicular to the pore axis (A) while they are parallel to the pore axis in the 35 nm pores (C). (B) Schematic 2D diffraction patterns from the LC columnar phase on the surface of the membrane (I) and inside 200 nm (II) and 35 nm (III) pores. *Bottom:* 1D-reduced intensity measured during the microfocus scan across the polymer-impregnated template (D). 2D μ XRD patterns measured on a PDES thin film close to the surface (thickness coordinate of 50 μm) and inside the nanoporous templates (125 μm) with 200 nm and 35 nm pore size, respectively (E). Pore axis is vertical.

The 2D GIWAXS patterns show that the majority of the lamellae are aligned perpendicular to the rubbing direction (Figure 1D), similarly to the case of PDES. At the same time, the X-ray measurements confirm the existence of orientational defects visualized on the AFM micrographs (see SI for more details). By increasing the side-chain length further (the case of PDHS, $n=6$), the columnar orientation does not vary anymore, according to X-ray diffraction (cf. Figure 1E) and AFM (cf. Figure 1K).

The behavior of PDAS deposited on PTFE-rubbed surfaces can be rationalized in terms of the mismatch between the unit cell parameters of the contact planes. PTFE forms hexagonal phase at room temperature, the so-called phase IV ($a = b = 5.6$

Å, $c = 19.5$ Å; helix 15₇).^[29] The analysis of the unit cell mismatch calculated for the form IV crystal of PTFE is given in Table 1. One can see that the backbones of PDAS and PTFE are parallel for the PDAS having the smallest lateral mismatch ($\leq 7.8\%$). Due to conformational defects in PDAS (conformationally-disordered mesophase) the register between the c -parameters of the unit cells can be disregarded. For the other three samples, *i.e.* PDES, PDPenS and PDHS, the preferential orientation on PTFE is perpendicular to the rubbing direction and was qualified as grapho-epitaxy. Noteworthy, AFM experiments performed on PDES have shown that the high quality orientation induced by PTFE rubbing can be maintained up to the film thicknesses of approximately one micron.

Table 1. Correlations between the mismatch of the columnar diameter of poly(di-*n*-alkylsiloxanes) and PTFE unit cell and their relative orientation

Sample	n ^a	PTFE		Relative orientation
		a, Å	Mismatch(%) with respect to a _{PTFE} =5.6 Å ^b	
PDES	2	9.3	21.9	⊥
PDPS	3	11.2	1.3	
PDBS	4	12.3	7.8	

PDPenS	5	13.6	16.6	⊥
PDHS	6	14.6	22.3	⊥

a) n – number of carbons in the alkyl side chain;

b) The mismatch values take into account the temperature effect of LC phase and thus correspond to the temperature at which the samples were analyzed.

To further explore such alteration between molecular epitaxy and grapho-epitaxy, we studied orientation of PDES embedded in inorganic nanoporous templates in which the epitaxial interaction with the substrate can be excluded. Geometrical constraints imposed by the pore walls of the template can

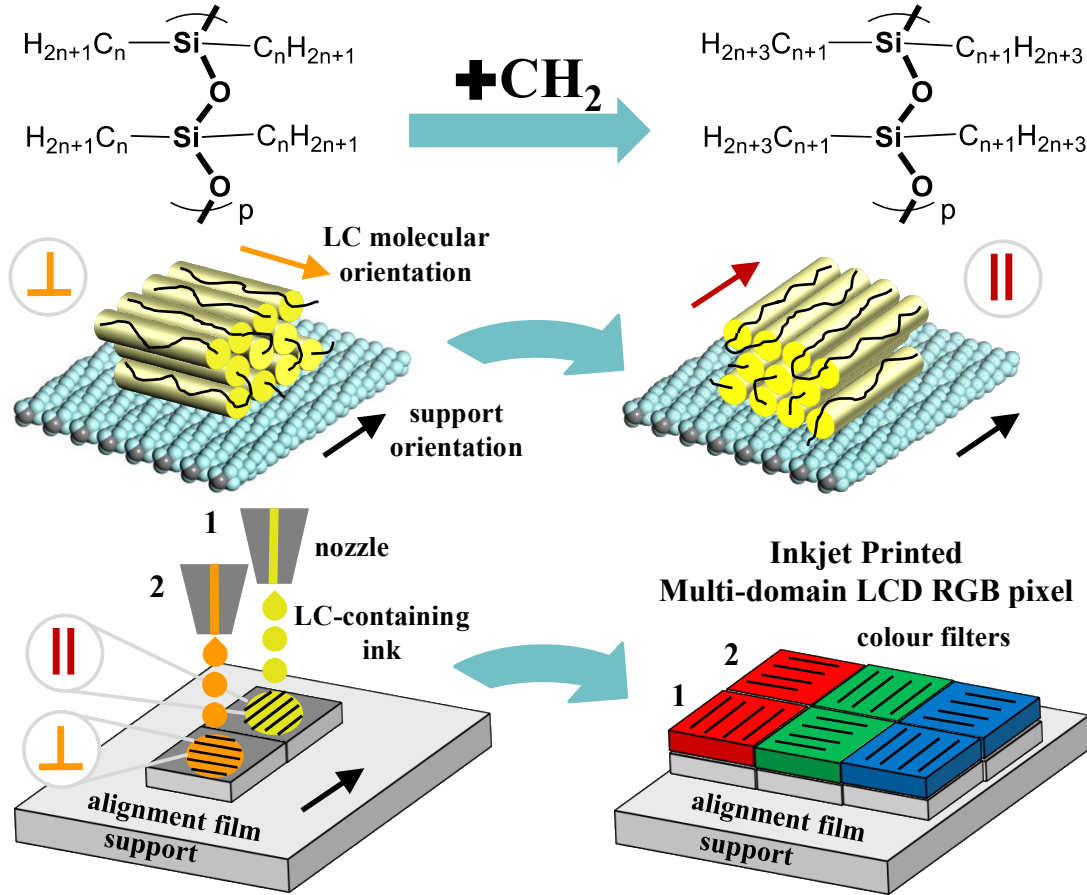


Figure 3. Schematics of the two mechanisms of the LC alignment in a series of model poly(di-*n*-alkylsiloxanes) PDAS: grapho-epitaxy (left) and molecular epitaxy (right). Addition of one CH₂ group to the side chain can change the macromolecular orientation by 90 degrees. Example of a multi-domain colour LCD where each pixel contains domains oriented according to the mechanisms of true molecular epitaxy and grapho-epitaxy. Such technology does not require buffing of the substrate for LC alignment and allows wider viewing angles.

efficiently confine semicrystalline polymers and discotic molecules.^{14,30,31} An anodic aluminum oxide (AAO) membrane can be used as a model support to induce LC alignment. We performed μ XRD scans across the AAO membrane (i.e., along its thickness axis) with 200 and 35 nm-sized pores impregnated with PDES sample, as shown in Figure 2. The 2D μ XRD patterns corresponding to free PDES film on top of the membrane and to that located inside the 200 nm pores are exemplified on Figure 2E (top and bottom left). The diffractogram corresponding to position of 50 μ m along the thickness

axis shows the 10 reflection corresponding to the intercolumnar distance of 9.3 Å located on the meridian of the pattern. Such orientation is similar to the one found above in thin films on PTFE-rubbed surface and can be viewed as the conventional in-plane orientation of PDES with 10_{hex} vector normal to the substrate (cf. Fig. 2A).²⁶ For PDES within the pores, the diffraction pattern is similar (cf. Figure 2B), which means that the molecular layers in the pore are preferentially in register with the PDES in the top layer. Therefore, for such a large pore diameter the interaction of the PDES with the pore walls is likely to be less important than the one with the PDES in

the top layer. However, when the pore size is decreased to 35 nm one observes inside the pores a six-spot pattern with diffraction peaks situated at 60° with respect to each other. A typical 2D diffractogram corresponding to a PDES film is shown on Figure 2E (bottom right). Such pattern prompts us suggesting that the grapho-epitaxy with the pore walls takes place. This means that now the conventional in-plane orientation is realized with the pore walls while the epitaxy with the PDES in the top layer is broken. In this case the mesomorphic lamellae grow strictly along the pore axis direction, *i.e.* with one of the 10_{hex} vectors of the columnar phase oriented perpendicular to the pore axis (see Figure 2B-C). Noteworthy, the same grapho-epitaxial orientation was also obtained for other polymers of the poly(*di-n*-alkylsiloxane) family, *i.e.* for PDPS, PDBS, PDPenS and PDHS. The main conclusion of this part of the study is that grapho-epitaxial interactions cause the mesomorphic lamellae orientation along the dominant topography features (*i.e.*, grooves) similarly to the case of PDAS on PTFE-rubbed substrates when the lattice mismatch is above ca. 7.8 %.

Taking into account that there is a high demand for new alternative methods of LC layer alignment for organic electronics and, in particular, for the LCD technology^[32,33], the reported alternating alignment mechanism of the model columnar LCs could be of potential interest to fabricate multi-domain LCD that have superior properties with respect to the traditional twisted-nematic (TN) LCDs. Various approaches have been reported to achieve a multi-domain alignment (MDA) including polymerization of reactive mesogen¹⁸ or inkjet-printed micro-protrusions,^[34] however, they are rather complex and challenging for the upscaling. Figure 3 shows a hypothetical example of a LC-based display with three pixels and RGB filters where each color pixel contains 2 subpixels with two mutually orthogonal LC orientations. Each subpixel could be deposited using inkjet printing. With the tendency of increasing the number of pixels per unit of display area, the future challenge could be to keep the LC orientation whilst moving from micro- to nanoscale. Importantly, in this case, the induction of two mutually orthogonal LC orientations becomes possible on the same rubbed substrate, which can facilitate the fabrication procedure and open new perspectives in the field of organic and printed electronics.

ASSOCIATED CONTENT

Supporting Information

The Supporting Information is available free of charge on the ACS Publications website.

Experimental section, table with characteristics of PDA sample, schematics of the experimental Grazing-Incidence and Micro-focus X-ray diffraction setups. (PDF)

AUTHOR INFORMATION

Corresponding Author

* Dimitri.Ivanov@uha.fr

Present Addresses

† Department of Chemistry, University College London, 20 Gordon Street, London, WC1H 0AJ, UK

‡ European Synchrotron Radiation Facility, 6 rue Jules Horowitz, Grenoble 38043, France

Author Contributions

The manuscript was written through contributions of all authors. All authors have given approval to the final version of the manuscript.

Funding Sources

Ministry of Education and Science of the Russian Federation (contract № 14.616.21.0072 from July 28, 2016 (RFMEFI61616X0072)).

ACKNOWLEDGMENT

D.A.I. acknowledges greatly thanks the Ministry of Education and Science of the Russian Federation (contract № 14.616.21.0072 from 28 July 2016 (RFMEFI61616X0072)) for financial support. The authors thank Prof. Martin Möller (DWI, Aachen, Germany) for donation of the PDAS samples. Authors are grateful to Dr. Vesna Stanic and Dr. Elaine DiMasi from the NSLS, BNL (USA) for the excellent technical support and for Manfred Burghammer from the ID13 beamline of the ESRF (Grenoble, France).

ABBREVIATIONS

PDAS - poly(*di-n*-alkylsiloxane); GIXD- Grazing-Incidence X-ray Diffraction.

REFERENCES

- (1) Takatoh, K.; Hasegawa, M.; Mitsuhiro, K.; Nltoh, O.; Hasegawa, R.; Sakamoto, M. *Alignment Technologies and Applications of Liquid Crystal Devices*; Taylor & Francis, 2005.
- (2) van Breemen, A. J. J. M.; Herwig, P. T.; Chlon, C. H. T.; Sweelssen, J.; Schoo, H. F. M.; Setayesh, S.; Hardeman, W. M.; Martin, C. a.; de Leeuw, D. M.; Valetton, J. J. P.; Bastiaansen, C. W. M.; Broer, D. J.; Popa-Merticaru, A. R.; Meskers, S. C. J. Large Area Liquid Crystal Monodomain Field-Effect Transistors. *J. Am. Chem. Soc.* **2006**, *128* (7), 2336–2345 DOI: 10.1021/ja055337l.
- (3) Shah, R. R.; Abbott, N. L. Principles for Measurement of Chemical Exposure Based on Recognition-Driven Anchoring Transitions in Liquid Crystals. *Science* **2001**, *293* (5533), 1296–1299 DOI: 10.1126/science.1062293.
- (4) Sen, A.; Acharya, B. R. Alignment of Nematic Liquid Crystals at Inorganic Salt–liquid Crystal Interfaces. *Liq. Cryst.* **2011**, *38* (4), 495–506 DOI: 10.1080/02678292.2011.553291.
- (5) Ong, H. L.; Hurd, A. J.; Meyer, R. B. Alignment of Nematic Liquid Crystals by Inhomogeneous Surfaces. *J. Appl. Phys.* **1985**, *57* (2), 186 DOI: 10.1063/1.334841.
- (6) Lee, K.; Paek, S.; Lien, A.; Durning, C.; Fukuro, H. Microscopic Molecular Reorientation of Alignment Layer Polymer Surfaces Induced by Rubbing and Its Effects on LC Pretilt Angles. *Macromolecules* **1996**, *29* (27), 8894–8899 DOI: 10.1021/ma960683w.
- (7) van Aerle, N. A. J. M.; Tol, A. J. W. Molecular Orientation in Rubbed Polyimide Alignment Layers Used for Liquid-Crystal Displays. *Macromolecules* **1994**, *27* (22), 6520–6526 DOI: 10.1021/ma00100a042.
- (8) Lee, B. W.; Clark, N. a. Alignment of Liquid Crystals with Patterned Isotropic Surfaces. *Science* **2001**, *291* (5513), 2576–2580 DOI: 10.1126/science.291.5513.2576.
- (9) Ikeno, H.; Oh-saki, A.; Nitta, M.; Ozaki, N.; Yokoyama, Y.; Nakaya, K.; Kobayashi, S. Electrooptic Bistability of a Ferroelectric Liquid Crystal Device Prepared Using Polyimide Langmuir-Blodgett Orientation Films. *Jpn. J. Appl. Phys.* **1988**, *27* (Part 2, No. 4), L475–L476 DOI: 10.1143/JJAP.27.L475.
- (10) Maret, G.; Blumstein, A. Orientation of Thermotropic Liquid-Crystalline Polyesters in High Magnetic Fields. *Mol. Cryst. Liq. Cryst.* **1982**, *88* (1–4), 295–309 DOI: 10.1080/00268948208072600.
- (11) Gopinadhan, M.; Majewski, P. W.; Osuji, C. O. Facile Alignment of Amorphous Poly(ethylene Oxide) Microdomains in a Liquid Crystalline Block Copolymer Using Magnetic Fields: Toward Ordered Electrolyte Membranes. *Macromolecules* **2010**, *43* (7), 3286–3293 DOI: 10.1021/ma9026349.

- (12) Kim, J.-H.; Yoneya, M.; Yokoyama, H. Tristable Nematic Liquid-Crystal Device Using Micropatterned Surface Alignment. *Nature* **2002**, *420* (6912), 159–162 DOI: 10.1038/nature01163.
- (13) Twomey, C.; Blanton, T.; Marshall, K.; Chen, S.; Jacobs, S. Some Dynamic Features of the Preparation of Liquid Crystalline Elastomers. *Liq. Cryst.* **1995**, *19* (3), 339–344 DOI: 10.1080/02678299508031990.
- (14) Steinhart, M.; Zimmermann, S.; Göring, P.; Schaper, A. K.; Gösele, U.; Weder, C.; Wendorff, J. H. Liquid Crystalline Nanowires in Porous Alumina: Geometric Confinement versus Influence of Pore Walls. *Nano Lett.* **2005**, *5* (3), 429–434 DOI: 10.1021/nl0481728.
- (15) Ha, K.; Ahn, H.; Son, C. Studies on the E7 Liquid Crystal Orientations Confined to Perfluorinated Carboxylic Acid-• treated Cylindrical Cavities of Anodise Membranes by FTIR Spectroscopy. *Liq. Cryst.* **2006**, *33* (8), 935–940 DOI: 10.1080/02678290600871440.
- (16) Castellano, J. A. Surface Anchoring of Liquid Crystal Molecules on Various Substrates. *Mol. Cryst. Liq. Cryst.* **1983**, *94* (1–2), 33–41 DOI: 10.1080/00268948308084245.
- (17) Stöhr, J.; Samant, M. G.; Cossy-Favre, A.; Diaz, J.; Momoi, Y.; Odahara, S.; Nagata, T. Microscopic Origin of Liquid Crystal Alignment on Rubbed Polymer Surfaces. *Macromolecules* **1998**, *31* (6), 1942–1946 DOI: 10.1021/ma9711708.
- (18) Jo, S. I.; Kim, J.-H.; Yu, C.-J. Multi-Domain Alignment of Liquid Crystal Using a Stamp of Anisotropic Morphology Fabricated by a Directional Polymerization of Reactive Mesogen. *Mol. Cryst. Liq. Cryst.* **2015**, *613* (1), 190–196 DOI: 10.1080/15421406.2015.1032734.
- (19) Bobrovsky, A.; Ryabchun, A.; Shibaev, V. Liquid Crystals Photoalignment by Films of Side-Chain Azobenzene-Containing Polymers with Different Molecular Structure. *J. Photochem. Photobiol. A Chem.* **2011**, *218* (1), 137–142 DOI: 10.1016/j.jphotochem.2010.12.013.
- (20) Wittmann, J. C.; Smith, P. Highly Oriented Thin Films of Poly(tetrafluoroethylene) as a Substrate for Oriented Growth of Materials. *Nature* **1991**, *352* (6334), 414–417 DOI: 10.1038/352414a0.
- (21) Yan, S.; Katzenberg, F.; Petermann, J.; Yang, D.; Shen, Y.; Straupé, C.; Wittmann, J. C.; Lotz, B. A Novel Epitaxy of Isotactic Polypropylene (α Phase) on PTFE and Organic Substrates. *Polymer (Guildf.)* **2000**, *41* (7), 2613–2625 DOI: 10.1016/S0032-3861(99)00310-9.
- (22) Fenwick, D.; Smith, P.; Wittmann, J. C. Epitaxial and Graphoepitaxial Growth of Materials on Highly Orientated PTFE Substrates. *J. Mater. Sci.* **1996**, *31* (1), 128–131 DOI: 10.1007/BF00355135.
- (23) Beekmans, L. G. M.; Valle, R.; Vancso, G. J. Nucleation and Growth of Poly(ϵ -Caprolactone) on Poly(Tetrafluoroethylene) by in-Situ AFM. **2002**, 9383–9390.
- (24) Geary, J. M.; Goodby, J. W.; Kmetz, a. R.; Patel, J. S. The Mechanism of Polymer Alignment of Liquid-Crystal Materials. *J. Appl. Phys.* **1987**, *62* (10), 4100 DOI: 10.1063/1.339124.
- (25) Out, G. J. J. Poly(di-N-Alkylsiloxane)s, Synthesis and Molecular Organization, University of Twente, The Netherlands, 1994.
- (26) Defaux, M.; Vidal, L.; Möller, M.; Gearba, R. I.; Dimasi, E.; Ivanov, D. A. Thin Films of a Main-Chain Columnar Liquid Crystal: Studies of Structure, Phase Transitions, and Alignment. *Macromolecules* **2009**, *42*, 3500–3509.
- (27) Gearba, R. I.; Dubreuil, N.; Anokhin, D. V.; Godovsky, Y. K.; Ruan, J.-J.; Thierry, A.; Lotz, B.; Ivanov, D. a. Role of Columnar Mesophase in the Morphological Evolution of Polymer Single Crystals upon Heating: A Combined Atomic Force Microscopy and Electron Diffraction Study. *Macromolecules* **2006**, *39* (3), 978–987 DOI: 10.1021/ma051606g.
- (28) Gearba, R. I.; Anokhin, D. V.; Bondar, A. I.; Godovsky, Y. K.; Papkov, V. S.; Makarova, N. N.; Magonov, S. N.; Wim Bras, O.; Koch, M. H. J.; Masin, F.; others. Mesomorphism, Polymorphism, and Semicrystalline Morphology of Poly (Di-N-Propylsiloxane). *Macromolecules* **2006**, *39* (3), 988–999.
- (29) Clark, E. S. The Crystal Structure of Polytetrafluoroethylene, Forms I and IV. *J. Macromol. Sci. Part B* **2006**, *45* (2), 201–213 DOI: 10.1080/00222340500522265.
- (30) Duran, H.; Steinhart, M.; Butt, H.-J.; Floudas, G. From Heterogeneous to Homogeneous Nucleation of Isotactic Poly(propylene) Confined to Nanoporous Alumina. *Nano Lett.* **2011**, *0*–4 DOI: 10.1021/nl200153c.
- (31) García-Gutiérrez, M.-C.; Linares, A.; Hernández, J. J.; Rueda, D. R.; Ezquerro, T. a; Poza, P.; Davies, R. J. Confinement-Induced One-Dimensional Ferroelectric Polymer Arrays. *Nano Lett.* **2010**, *10* (4), 1472–1476 DOI: 10.1021/nl100429u.
- (32) Galstian, T. Surface Programming Method and Light Modulator Devices Made Thereof. WO2010006419, January 21, 2010.
- (33) Kuroda, T. Liquid Crystal Layer Forming Ink Composition, and Optical Film, Polarizing Film and Liquid Crystal Display Produced with the Ink Composition. US20090033834, February 5, 2009.
- (34) Park, S. W.; Lim, S. H.; Choi, Y. E.; Jeong, K.-U. U.; Lee, M.-H. H.; Chang, H. S.; Kim, H. S.; Lee, S. H. Multi-Domain Vertical Alignment Liquid Crystal Displays with Ink-Jet Printed Protrusions. *Liq. Cryst.* **2012**, *39* (4), 501–507 DOI: Doi 10.1080/02678292.2012.657697.

Insert Table of Contents artwork here

